

Supplementary Materials for

Identification of TNFR2 and IL-33 as therapeutic targets in localized fibrosis

David Izadi, Thomas B. Layton, Lynn Williams, Fiona McCann, Marisa Cabrita, Ana I. Espirito Santo, Weilin Xie, Marco Fritzsche, Huw Colin-York, Marc Feldmann, Kim S. Midwood, Jagdeep Nanchahal*

*Corresponding author. Email: jagdeep.nanchahal@kennedy.ox.ac.uk

Published 4 December 2019, *Sci. Adv.* **5**, eaay0370 (2019)

DOI: 10.1126/sciadv.aay0370

This PDF file includes:

- Fig. S1. DD is a localized inflammatory disorder.
- Fig. S2. Single-cell RNA-seq of immune cells from freshly isolated Dupuytren's nodules.
- Fig. S3. Mast cells and M2 macrophages are the predominant sources of TNF in DD.
- Fig. S4. TNF induced protein expression and TNF receptor expression in Dupuytren's cord.
- Fig. S5. IL-33 and its receptor ST2 are expressed on Dupuytren's myofibroblasts.
- Fig. S6. No reduction in cell viability following treatment with neutralizing antibodies.
- Fig. S7. siRNA knockdown validation for *TNFRSF1A*, *TNFRSF1A*, and *ST2*.
- Fig. S8. IL-33 and TNF stromal-immune cell cross-talk in DD.

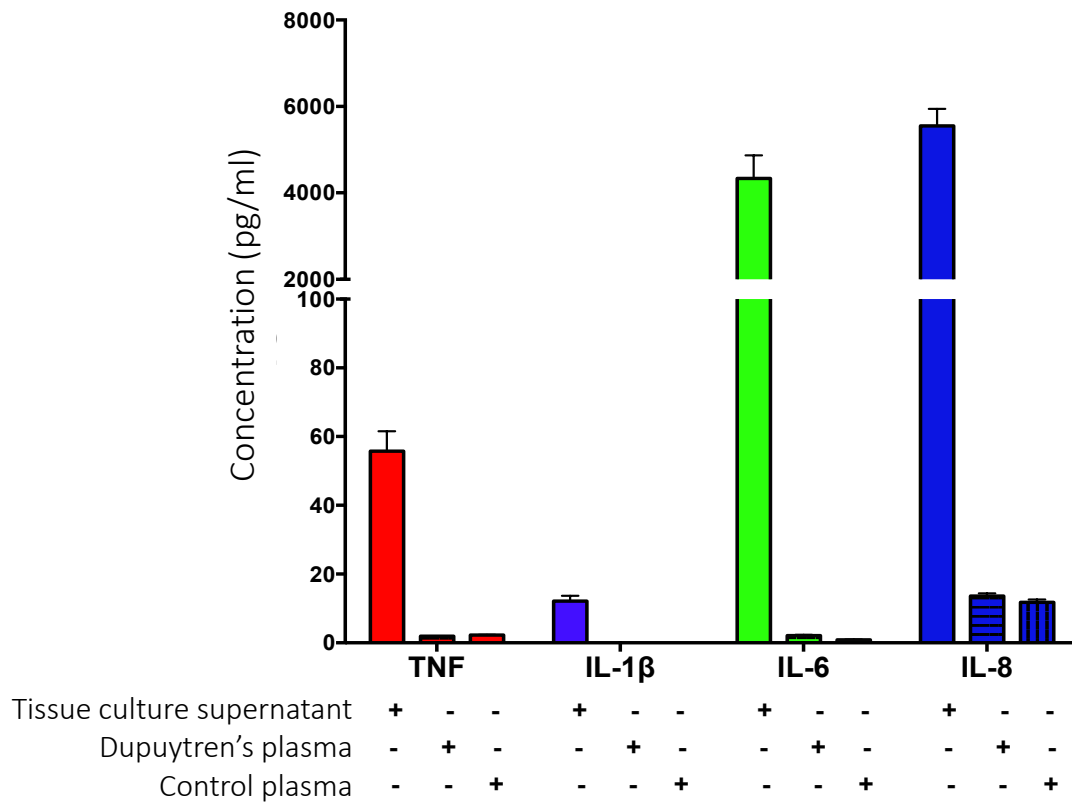


Fig. S1. DD is a localized inflammatory disorder. Bar plot of cytokines in plasma of DD patients compared to levels in freshly disaggregated nodular cells (tissue culture supernatant) and plasma from individuals (control plasma) not affected by DD ($n = 35$ independent donors).

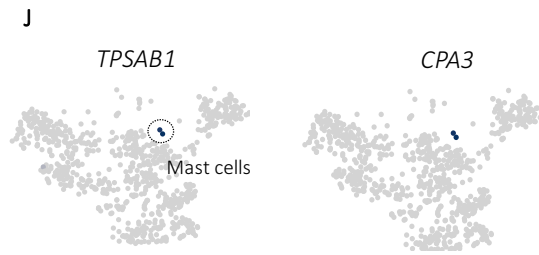
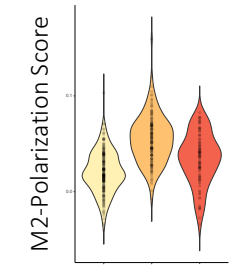
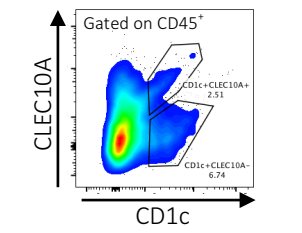
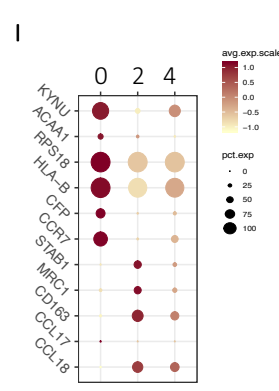
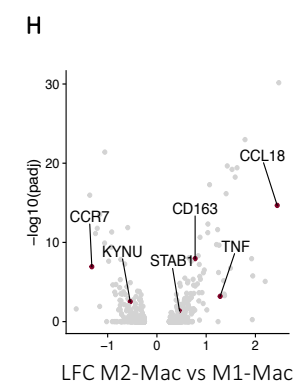
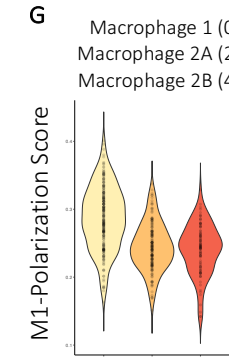
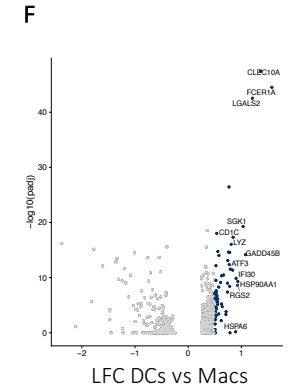
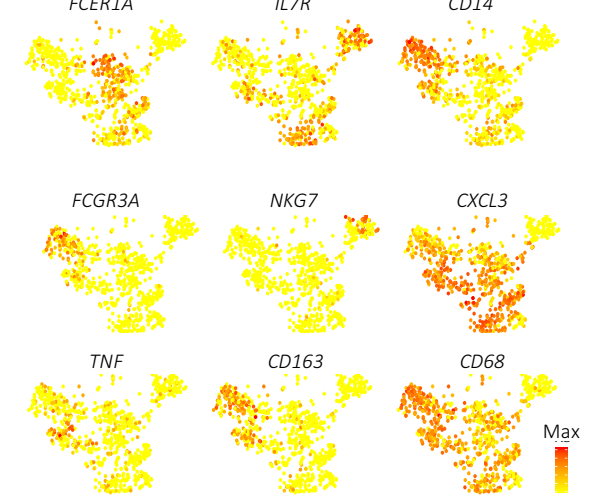
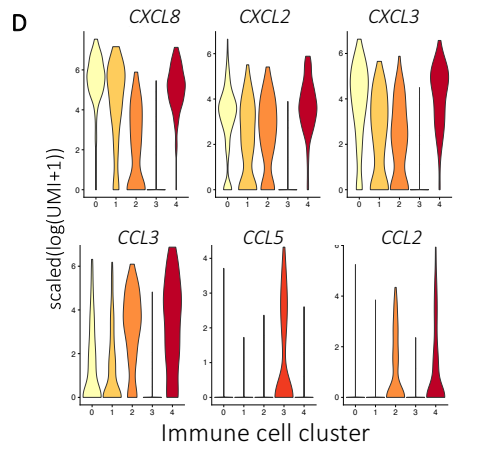
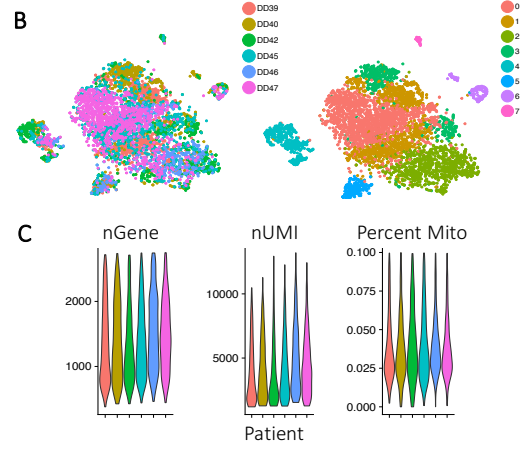
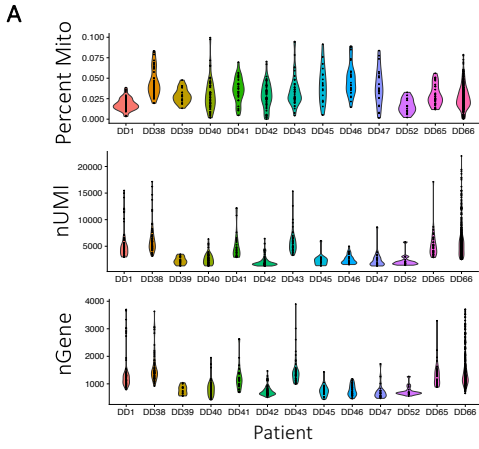


Fig. S2. Single-cell RNA-seq of immune cells from freshly isolated Dupuytren's nodules. (A) Violin plots showing quality control metrics for single-cell RNA-seq of immune cells in DD nodules ($n = 12$ DD patients, $k = 1,033$ cells). (B) tSNE embeddings of single cell RNA-seq of nodular cells coloured by patient donor (DD39-DD47) and Louvain cluster (0-7). (C) Violin plots showing quality control metrics for each DD patient ($n = 6$ DD patients, $k = 7,332$ cells). (D) Violin plots showing chemokine gene expression in scaled($\log(\text{UMI}+1)$) in immune clusters. (E) tSNE embeddings of immune cells in DD nodules showing cell marker gene expression in scaled($\log(\text{UMI}+1)$). (F) Top panel: Volcano plot showing differentially expressed genes (Wilcoxon Rank Sum test) between dendritic cell cluster and myeloid clusters. FDR-corrected (BH correction) p-value. Bottom panel; Representative density plots of flow cytometry analysis showing $\text{CD45}^+\text{CD1C}^+\text{CLEC10A}^{+/-}$ immune cells in freshly disaggregated DD nodules. (G) Violin plot for 'M1 and M2-macrophage polarization score' in three macrophage clusters. This score represents the scaled average expression of the test gene sets ($n = 198$ and $n = 462$ genes). (H) Volcano plot showing differentially expressed genes (Wilcoxon Rank Sum test) between M2-macrophage (2A-B) clusters and M1-macrophage cluster. FDR-corrected (BH correction) p-value. (I) Dot plot showing gene expression in macrophage clusters in scaled($\log(\text{UMI}+1)$). Pct.exp = percentage of cells expressing gene. (J) tSNE embeddings of immune cells showing expression of mast cell marker genes in scaled($\log(\text{UMI}+1)$). Two mast cells highlighted.

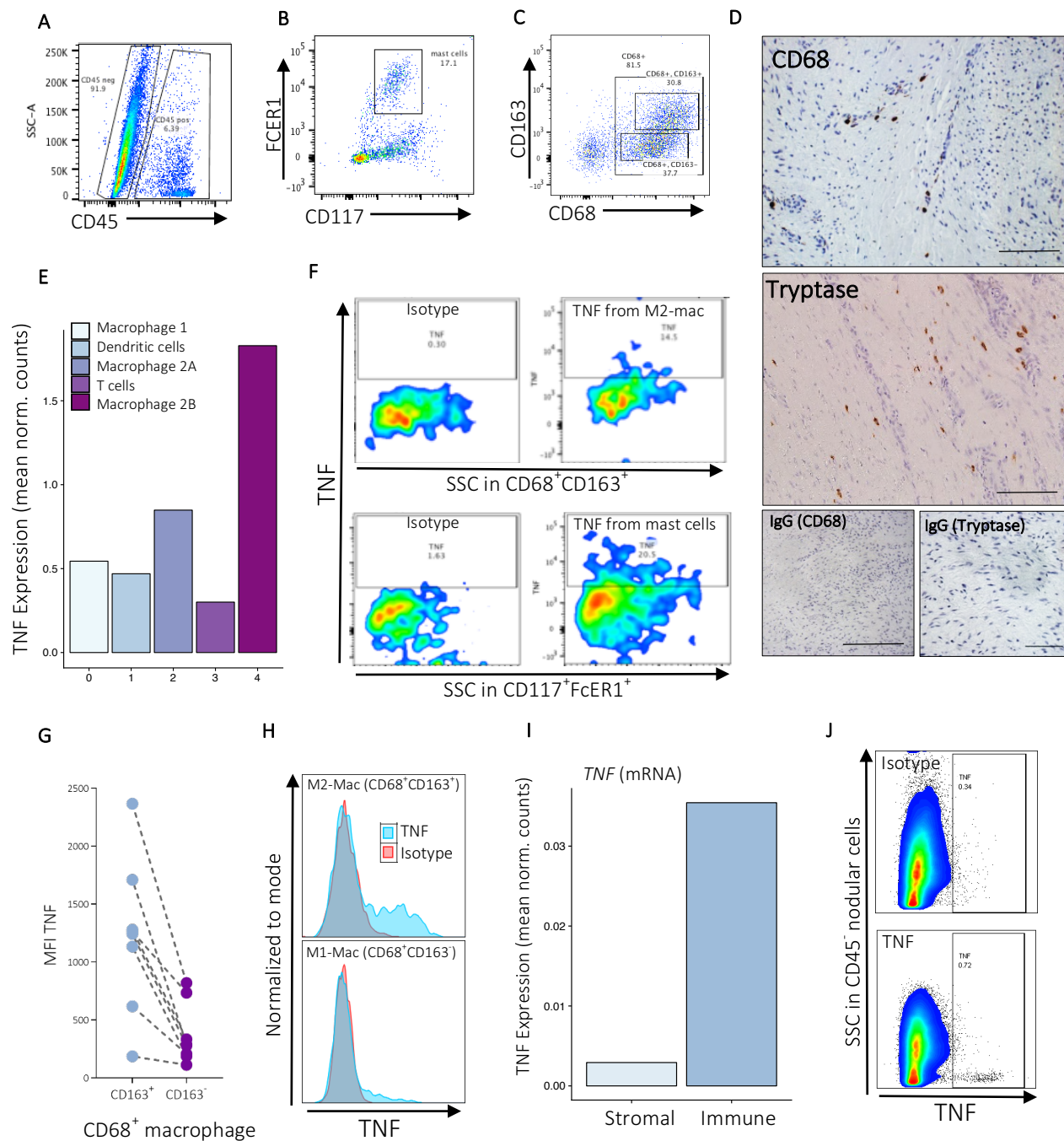


Fig. S3. Mast cells and M2 macrophages are the predominant sources of TNF in DD. (A) Scatter plot of flow cytometry gating strategy on CD45⁺ in freshly isolated nodular cells ($n = 5$ DD patients). (B) Scatter plot of flow cytometry gating strategy on CD45⁺FCER1⁺CD117⁺ mast cells in DD nodules. (C) Scatter plot of flow cytometry gating strategy on CD45⁺CD68⁺CD163^{+/-} macrophages in freshly isolated nodular cells. (D) Representative images of immunohistochemistry for tryptase⁺ mast cells and CD68⁺ macrophages in DD nodules, with isotype control. Scale bar = 40 μm (top two panels) and 20 μm (bottom two panels). (E) Bar plot of *TNF* gene expression in immune cell clusters in single cell RNA-seq. Expression in average normalized counts per cell cluster. (F) Representative density plots of flow cytometry analysis showing TNF expression in mast cells and macrophages ($n = 5$ DD patients). (G) Line plot of flow cytometry analysis showing TNF expression (MFI) in CD163⁺ and CD163⁻ macrophages ($n = 7$ DD patients). (H) Representative histograms of flow cytometry analysis for TNF expression in CD163⁻ and CD163⁺ macrophages in freshly disaggregated nodules with isotype control ($n = 5$ DD patients). (I) Bar plot of *TNF* gene expression in stromal cells and immune cells in single cell RNA-seq. Expression in average normalized counts per cluster. (J) Representative density plots of flow cytometry analysis showing TNF expression in CD45⁻ stromal cells in freshly disaggregated nodules with isotype control ($n = 6$ DD patients).

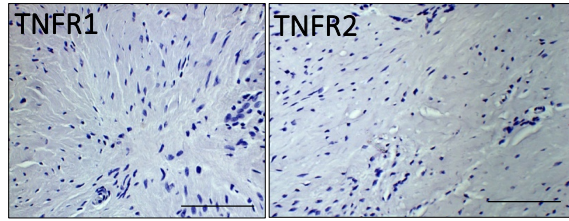
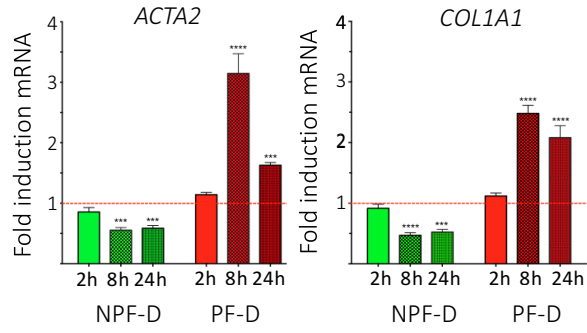
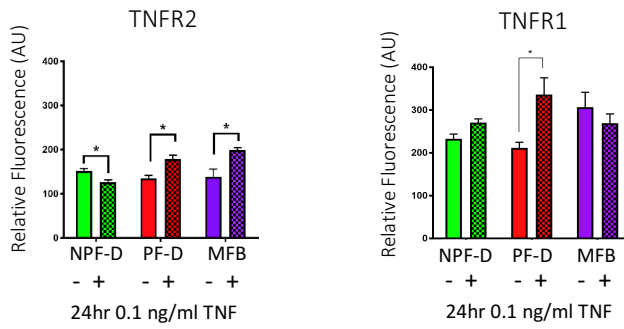
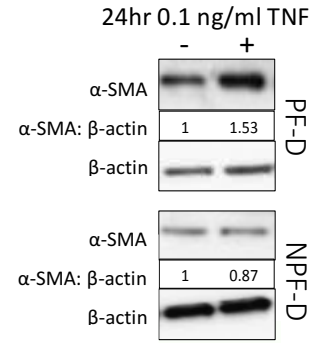
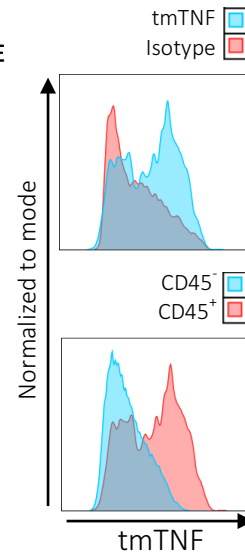
A**B****D****C****E**

Fig. S4. TNF induced protein expression and TNF receptor expression in Dupuytren's cord. (A)

Representative images of immunohistochemistry for TNFR1 and TNFR2 expression in Dupuytren's cord.

Scale bar = 20 μ m. **(B)** Bar plots of *ACTA2* and *COL1A1* gene expression in palmar (PF-D) and non-

palmar (NPF-D) dermal fibroblasts from DD patients treated with 0.1 ng/ml rTNF at 2, 8 and 24 hours

(h). ($n = 5$ DD patients, mean \pm SEM). **(C)** Western blot analysis showing α -SMA protein expression in

NPF-D and PF-D on treatment with 0.1 ng/ml rTNF. **(D)** Bar plots of quantitative immunofluorescence

for TNFR1 and TNFR2 protein expression in non-palmar (NPDF) and palmar (PDF) dermal fibroblasts

and myofibroblasts from DD patients on treatment with 0.1 ng/ml rTNF ($n = 5$ DD patients, mean \pm

SEM). **(E)** Representative histogram plots of flow cytometry analysis for transmembrane TNF expression

in freshly disaggregated DD nodular cells ($n = 4$ DD patients). * $P < 0.05$, ** $P < 0.01$, *** $P < 0.001$,

**** $P < 0.0001$.

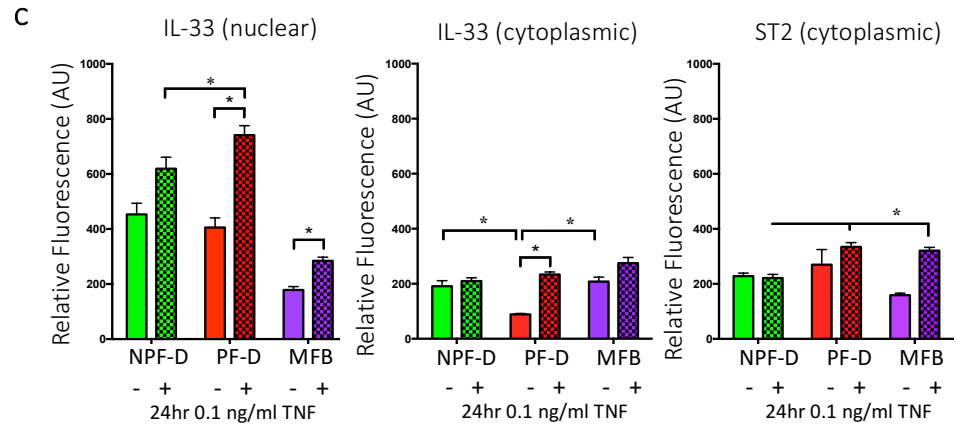
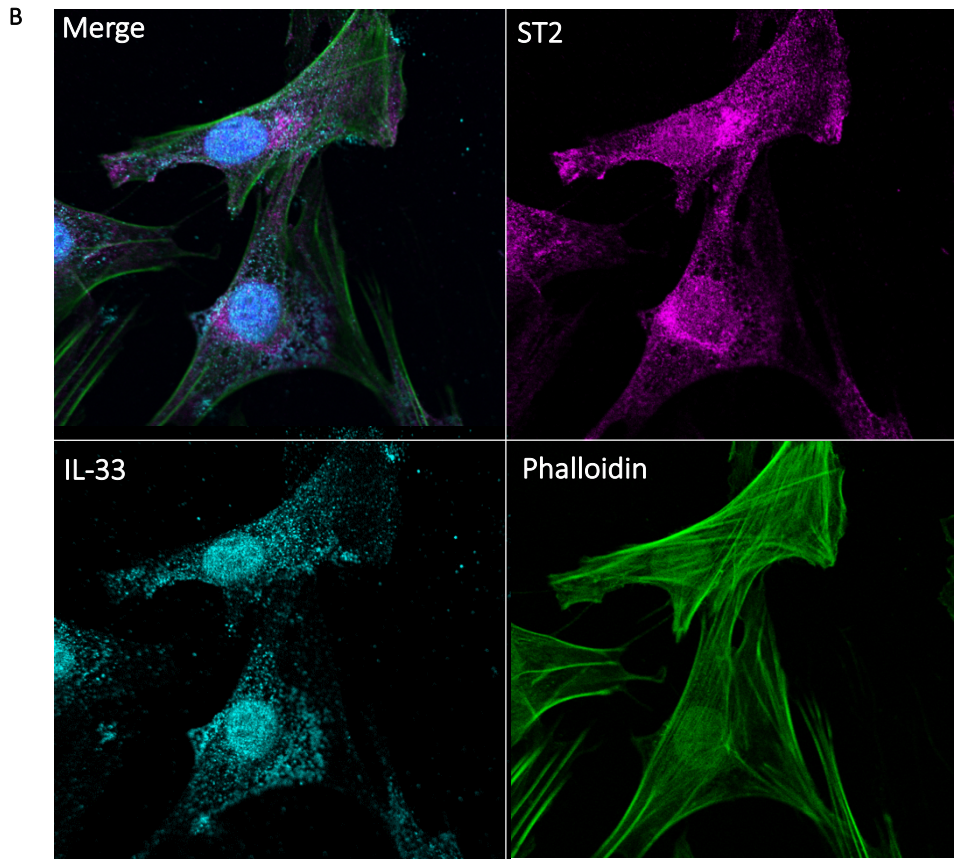
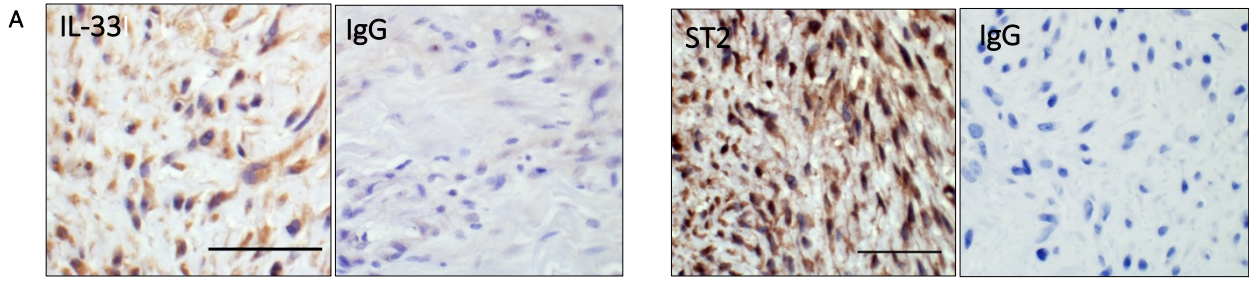


Fig. S5. IL-33 and its receptor ST2 are expressed on Dupuytren's myofibroblasts. (A) Representative images of immunohistochemistry for IL-33 and the receptor ST2 expression with corresponding isotype controls in DD nodules. Scale bar = 20 μm . (B) Representative confocal images of immunofluorescence for ST2 and IL-33 in freshly isolated myofibroblasts from DD nodules. Scale bar = 10 μm . (C) Bar plots of quantitative immunofluorescence showing cytoplasmic and nuclear IL-33 staining and ST2 cytoplasmic staining in non-palmar (NPDF) and palmar (PDF) dermal fibroblasts and myofibroblasts from DD patients on treatment with 0.1 ng/ml rTNF ($n = 5$ DD patients, mean \pm SEM).

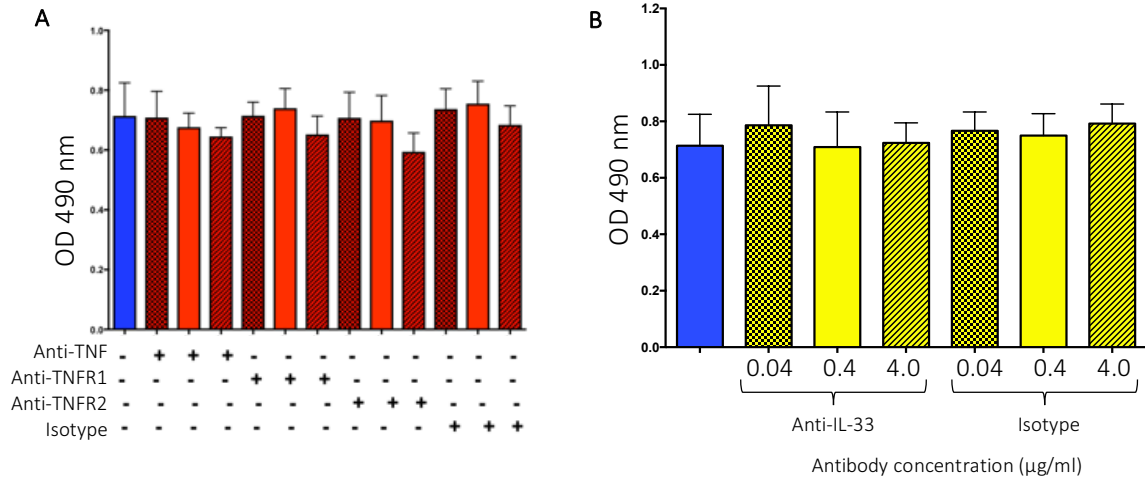


Fig. S6. No reduction in cell viability following treatment with neutralizing antibodies. (A) Bar plot of MTS cell viability assay of myofibroblasts treated over 24 hours with 1, 10 and 100 µg/ml of neutralizing anti-TNF, anti-TNFR1, anti-TNFR2 antibodies and isotype control. ($n = 3$ DD patients, in triplicate, mean \pm SEM). (B) Bar plot of MTS cell viability assay of myofibroblasts treated over 24 hours with 0.04, 0.4 and 4 µg/ml of neutralizing anti-IL-33 and isotype control. ($n = 3$ DD patients, in triplicate, mean \pm SEM). OD = Optical density.

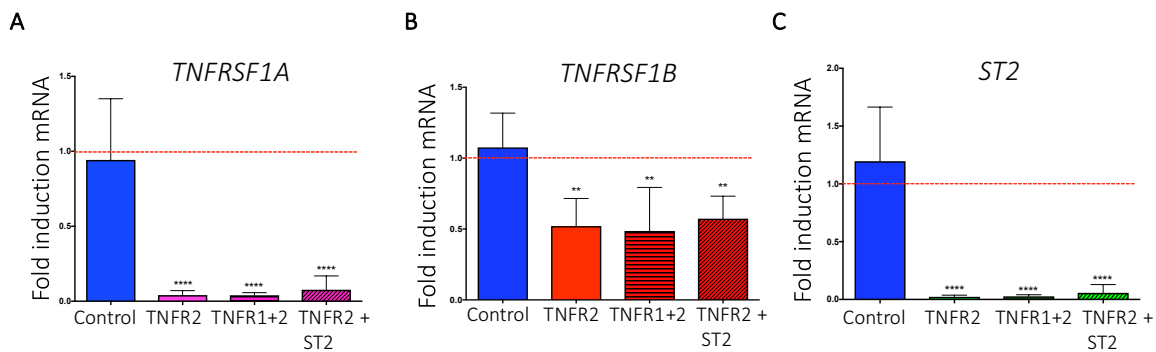


Fig. S7. siRNA knockdown validation for *TNFRSF1A*, *TNFRSF1A*, and *ST2*. (A-C) Bar plots of qPCR analysis showing gene expression of labelled genes following siRNA mediated knockdowns. ($n = 3$ DD patients, in triplicate, mean \pm SEM). $P < 0.05$, $**P < 0.01$, $***P < 0.001$, $****P < 0.0001$.

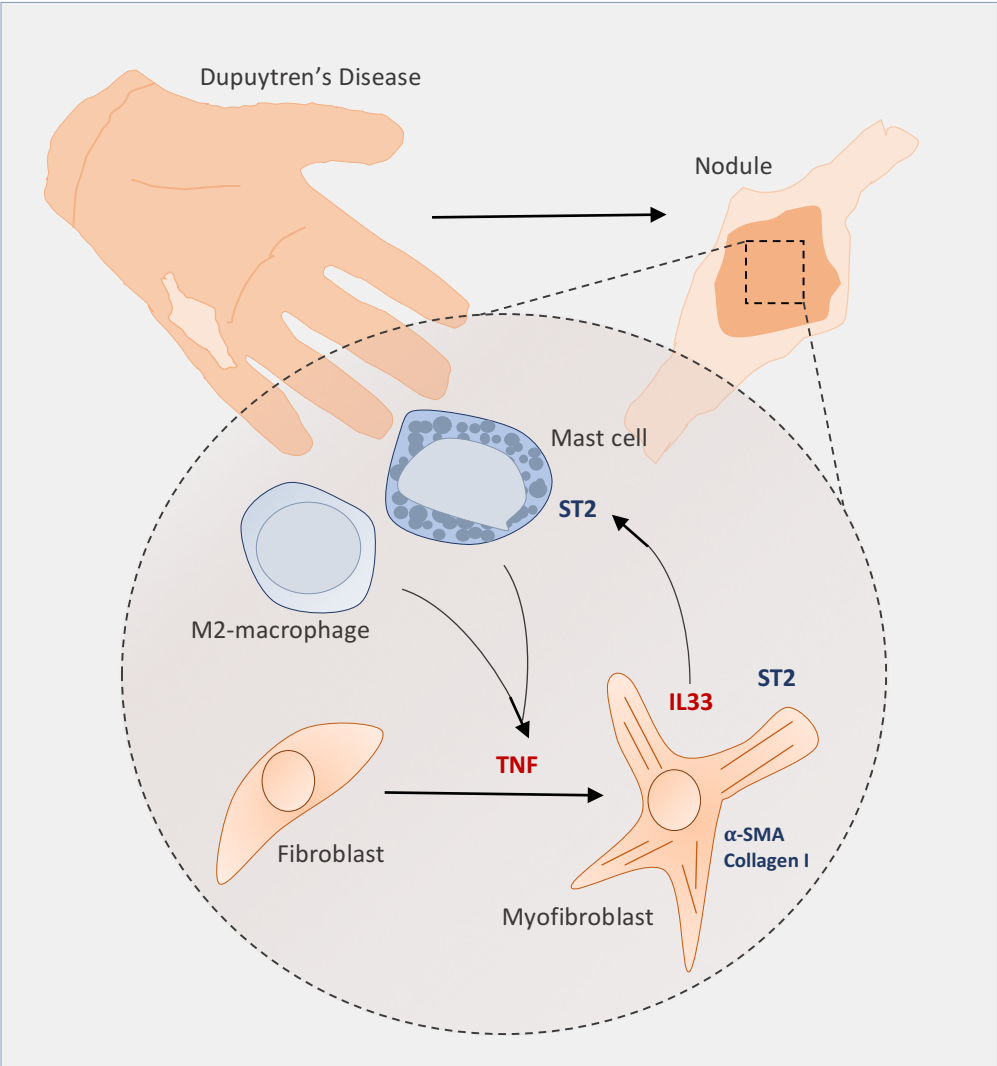


Fig. S8. IL-33 and TNF stromal-immune cell cross-talk in DD. Schematic illustrating that immune cells (mast cells and M2-macrophages) are the predominant source of TNF in DD that stimulates the development of the myofibroblast phenotype. Myofibroblasts are a significant source of IL-33 which further activates TNF secretion from immune cells.